INTRODUCTION TO NUCLEAR RESONANCE SYNCHROTRON RADIATION*

W. Sturhahn E. E. Alp, T. S. Toellner, P. Hession, M. Hu, and J. Sutter
Experimental Facilities Division
Advanced Photon Source, Argonne National Laboratory
Argonne, IL 60439

August 1997

To be presented at ICAME'97, International Conference on the Applications of The Mössbauer Effect, Rio de Janeiro, Brazil, September 14-20, 1997.

*This work is supported by the U.S. Department of Energy, Basic Energy Sciences-Materials Sciences, under contract #W-31-109-ENG-38.

DISCLAIMER

Introduction to Nuclear Resonant Scattering with Synchrotron Radiation

W. Sturhahn, E. E. Alp, T. S. Toellner, P. Hession, M. Hu, and J. Sutter
Advanced Photon Source, Argonne National Laboratory,
Argonne, Illinois 60439, USA

The concepts leading to the application of synchrotron radiation to elastic and inelastic nuclear resonant scattering are discussed. The resulting new experimental techniques are compared to conventional Mössbauer spectroscopy. A survey of situations that favor experiments with synchrotron radiation is offered.

In recent years, the use of synchrotron radiation has enjoyed increasing interest in applications to topics of Mössbauer spectroscopy [1, 2]. The development was initiated by the pioneering experimental work of Gerdau et al. [3] following the original proposal of Ruby [4] to use synchrotron radiation for the excitation of low-energy nuclear resonances. From the early experiments it was clear that synchrotron radiation experiments with nuclear resonances would only succeed if familiar energy-resolved measurements were replaced with a new time-resolved technique. During the last decade, we experienced the refinement of this novel method for obtaining hyperfine parameters. This exciting development materialized because of more intense synchrotron radiation sources at the European Synchrotron Radiation Facility (ESRF) [5] and at the Advanced Photon Source (APS) [6], powerful new avalanche photo diode detectors [7, 8, 9], and improved high-energy-resolution monochromators [10, 11, 12, 13]. Simultaneously the tools for evaluation of the novel time spectra were created, e.g., Sturhahn and Gerdau [14] developed extensive computer codes[1] based on the theoretical descriptions of Hannon and Trammel [15]. Many beautiful demonstrations of the basic features of the coherent elastic scattering channel using Bragg- and Laue-reflections from single crystals deepened the understanding of nuclear resonant scattering.

The effect of noncrystalline resonant materials inserted into the radiation path was initially studied by van Bürck et al. [16], but a simpler approach aiming at applications of the novel technique was suggested by Hastings et al. [17]. With newly developed instrumentation they were able to observe nuclear forward scattering of synchrotron radiation in analogy to conventional Mössbauer-transmission experiments. This approach, in combination with the deeper understanding of the phenomenon that was developed in the single-crystal experiments, evolved into a promising application. At present we can concede considerable progress towards a viable form of synchrotron Mössbauer spectroscopy (SMS) performed with the typical Mössbauer sample [18]. However, we also realize that SMS besides having undisputable advantages has limitations, mainly for technical reasons but nevertheless very real. Both topics will be addressed in this paper, and thus we hope to provide certain guidelines in the planning of experiments at synchrotron radiation

[1] the "CONUSS" software can be obtained from the corresponding author.

beamlines.

Besides the extention of conventional, i.e., energy-resolved, Mössbauer spectroscopy into the time domain, the advent of powerful synchrotron radiation sources permitted nuclear resonant scattering to establish a stronghold in a quite different area of condensed matter physics, i.e., the determination of phonon density of states. Although the theoretical groundwork for this exciting opportunity was prepared early [19, 20], it was impossible to carry out the experiment for lack of intensity and tunability of radioactive sources. Soon after the observation of inelastic nuclear resonant scattering by Seto et al. [21], it was demonstrated by Sturhahn et. al [22] that the technique provides unique information about the phonon density of states of the resonant isotope. The PHOENIX-technique (PHOnon Excitation by Nuclear Inelastic absorption of X-rays) is also well suited to provide Lamb-Mössbauer factors and second-order Doppler shifts [22, 23, 24, 25, 26]. In this paper, we will emphasize the capability of PHOENIX to provide valuable information for Mössbauer spectroscopy.

Sources for nuclear resonant scattering. – Synchroton radiation and γ-rays emitted by a radioactive source have such different properties that an explanantion is in order as to why they both permit Mössbauer experiments. In synchrotron radiation sources, ultrarelativistic electrons or positrons are kept in a storage ring in a closed orbit. They emit intense radiation due to acceleration while traversing bending magnets or periodic magnetic structures, such as undulators. The charged particles are not distributed evenly in their orbit but can only occupy certain stable positions, or buckets. Buckets that are actually filled with particles are called bunches, and the number and the separation of the bunches in a storage ring determine the time structure of the synchrotron radiation. The minimum separation and the length of the bunches depend on the storage ring design. The bunching of the electrons or positrons is a general feature of all storage rings, therefore the synchrotron radiation is emitted in short intense pulses that repeat periodically. On the contrary, the emission of photons from a radioactive nucleus is random in time.[2] The situation is inverted if we analyze the energy bandwidth of both sources, which is of the order of keV for the synchrotron radiation but only about the natural linewidth for a Mössbauer source. This reciprocal behavior prompts the conclusion that the experimental techniques should be similarly reciprocal, i.e., energy-resolved spectroscopy with radioactive sources and time-resolved spectroscopy with synchrotron radiation, which is illustrated in fig. 1.

A fair comparison of the relevant intensity provided by either source has to consider the particular method of measurement, i.e., energy resolved or time resolved. A commercially available ^{57}Co source with 10 mCi activity produces an equivalent spectral photon flux of approximately $2.5 \cdot 10^9$ ph/s/eV into $2 \times 2\,\mathrm{deg}^2$ solid angle (0.006 sr) if the range of the measurement covers 200 natural linewidths. Including losses in the optical elements, an undulator beamline at the APS provides about $2.5 \cdot 10^{12}$ ph/s/eV into $0.001 \times 0.003\,\mathrm{deg}^2$ solid angle ($3 \cdot 10^{-9}$ sr.) If samples are small, i.e., they only accept radiation within a small spatial or angular range, it is particularly useful to know brightness (spectral flux

[2] Coincidence techniques are not feasible because of severe reduction of useful intensity.

per solid angle) and brilliance (spectral flux per solid angle and per area) of the source. For the radioactive source. we obtain a brightness of $2.5 \cdot 10^{13}$ ph/s/(eV sr), and, at 30 cm distance, the brilliance is $2.2 \cdot 10^{7}$ ph/s/(eV sr mm^2). As perhaps expected synchrotron radiation achieves much higher values providing a brightness of $8.3 \cdot 10^{21}$ ph/s/(eV sr) and a brilliance of typically $4 \cdot 10^{21}$ ph/s/(eV sr mm^2). Evidently synchrotron radiation produces more useful intensity for Mössbauer experiments.

Other important characteristics are the best resolution obtainable and the maximum range achievable. The energy resolution of the radioactive source is given by the natural linewidth, and the maximum energy range obtained by Doppler-shifting techniques is typically 10^{-4} eV. In the case of synchrotron radiation, we have to analyze the situation with respect to a time-resolved measurement. The energy resolution relates to the recordable period of time that follows the excitation of the sample by a flash of synchrotron radiation. This time period is given by the bunch separation and is therefore subject to the operational mode of the storage ring. The energy resolution of the radioactive source will be exceeded if the bunch separation is larger than the lifetime of the excited nuclear state. The maximum energy range that is probed by the time spectrum follows from the time resolution of the detector, presently about 1 ns, and is about $7 \cdot 10^{-7}$ eV. Although SMS is not useful if large hyperfine splittings are expected, superior resolution can be obtained.

The polarization of the emitted radiation is an important property of the source. Essentially all applications of conventional Mössbauer spectroscopy use radioactive sources that emit unpolarized radiation. The mechanism producing synchrotron radiation guarantees almost complete linear polarization. In addition, optical elements can convert synchrotron radiation to circularly polarized radiation with high efficiency. In Table 1, we summarized the results of our comparison reflecting the unique properties of synchrotron radiation.

Synchrotron Mössbauer Spectroscopy. – The particular properties of synchrotron radiation promote a time-resolved method of measurement. The sample is illuminated with radiation pulses at well-known times, which are usually derived from operational control of the storage ring. Simultaneously a synchronized timing system receives input from a detector that observes radiation transmitted through the sample. Events occurring with certain time delays with respect to the incident synchrotron radiation pulses indicate the excitation of resonant nuclei. In general, such a time spectrum shows oscillations that are related to the hyperfine interactions of the nuclei. Also the lifetime of the nuclear excited state causes a characteristic decay, which may be greatly enhanced for thick samples.

The previously described method, known as "nuclear forward scattering" [17], utilizes coherent elastic scattering of the nuclei into the direction of the incident radiation. This situation was identified as a special case of the more general treatment of the "dynamical theory of Mössbauer optics" [15]. A unified understanding of energy-resolved Mössbauer spectroscopy and SMS can be developed with the index-of-refraction model [27]. Homogenous materials are characterized by energy-dependent indices of refraction that have 2×2-matrix representations owing to anisotropy with respect to the polarization of the radiation. Considering only the nuclear resonant part, we may write the index of

refraction, $n(\omega)$, as

$$n(\omega) = \frac{F\,\sigma\,\rho\,c}{2\omega} \sum_j \frac{\beta_j}{2\tau\,(\omega_j - \omega) - \mathrm{i}} \ , \tag{1}$$

where F is the Lamb–Mössbauer factor, σ is the nuclear resonant cross section, ρ is the density of the resonant nuclei, and τ is the lifetime of the excited nuclear state. $\hbar\omega_j$ are the energies and β_j, $\beta_j^\dagger = \beta_j$, $\sum_j \beta_j = 1$ are the weights of the individual nuclear transitions. For simplicity, we neglected the electronic contribution, as well as the vacuum contribution, which are isotropic and energy independent near nuclear resonances. The symmetries of the matrix are directly related to the hyperfine interactions in the material. When plane monochromatic waves with wave number k_0 and amplitudes $\tilde{\mathbf{A}}_0(\omega)$ pass through a platelet of thickness D, the transmitted amplitudes are

$$\tilde{\mathbf{A}}(\omega) = \mathrm{e}^{\mathrm{i}k_0 D\,n(\omega)}\,\tilde{\mathbf{A}}_0(\omega) \ . \tag{2}$$

Placing such a material in front of a Mössbauer source and observing the transmitted intensity versus the Doppler shift of the source resembles the well–known Mössbauer transmission experiment. The convolution of the material's response with the Lorentzian spectrum of the source provides the normalized transmission

$$S(\omega) = \frac{\tau}{\pi} \int \frac{\mathrm{trace}[\mathrm{e}^{-\mathrm{i}k_0 D\,n^\dagger(\omega')}\mathrm{e}^{\mathrm{i}k_0 D\,n(\omega')}]}{4\tau^2(\omega-\omega')^2+1}\,d\omega' \ . \tag{3}$$

This expression, the "transmission integral", was derived by Margulies and Ehrmann [28] and is paramount to the analysis of conventional Mössbauer spectra. They also pointed out that the effective thickness $\eta = F\,\sigma\,\rho\,D$ is critical to the observed line broadening in the Mössbauer spectrum.

The expression for the time dependence of a plane wave with wave number k_0 and amplitude $\mathbf{A}_0(t)$ after passing a platelet of thickness D is

$$\mathbf{A}(t) = \int R(t-t')\,\mathbf{A}_0(t')\,dt' \ . \tag{4}$$

The response function $R(t)$ of the platelet is related to the index of refraction by a Fourier transformation

$$R(t) = \frac{1}{2\pi} \int \mathrm{e}^{\mathrm{i}k_0 D\,n(\omega)}\,\mathrm{e}^{-\mathrm{i}\omega t}\,d\omega \ . \tag{5}$$

This expression is more conveniently written as $R(t) = \delta(t) + N(t)$, which explicitly shows prompt and delayed contributions. Furthermore the amplitudes of synchrotron radiation pulses incident on the platelet are well localized in time because the corresponding energy bandwidth $\hbar\Omega$ is several orders of magnitude larger than the hyperfine splitting.[3] We also associate a polarization unit vector $\mathbf{a}_0$ with the synchrotron radiation and normalize by $\int |\mathbf{A}_0(t)|^2\,dt = 1$ to obtain the time–dependent transmission

$$T(t) = |\mathbf{A}_0(t)|^2 \left\{1 + \frac{2}{\Omega}\,\mathrm{Re}[N(0)]\right\} + \frac{1}{\Omega}|N(t)\mathbf{a}_0|^2 \ . \tag{6}$$

[3] We assume rectangular shape for the energy spectrum of the synchrotron radiation.

The second term is commonly used to describe "nuclear forward scattering," and we will continue with a comparison of time-dependent and energy-dependent transmission functions.

A precise determination of hyperfine interactions benefits from thin absorbers for which the thickness broadening is negligible. We will study this case of small effective thickness by providing expansions in η of eqs. 3 and 6. For energy-resolved Mössbauer spectroscopy, the lowest order term is linear and the well-known sum of Lorentzians is recovered

$$S(\omega) \approx 1 - \frac{\eta}{4} \sum_j \frac{\mathrm{trace}[\beta_j]}{\tau^2(\omega - \omega_j)^2 + 1} \ . \tag{7}$$

An inspection of the time-dependent counterpart reveals a prompt response for terms linear in η, and the delayed emission into the forward direction is approximated by the second-order term, which is given by[4]

$$T_2(t) \approx \frac{\eta^2}{16\Omega\tau^2} \mathrm{e}^{-t/\tau} \sum_{j,l} \mathrm{e}^{-\mathrm{i}\omega_{jl}t} \mathbf{a}_0^* \beta_j \beta_l \mathbf{a}_0 \ . \tag{8}$$

The natural decay is modulated by oscillations with frequencies $\omega_{jl} = \omega_j - \omega_l$, and the number of possible frequencies can be large particularly for mixtures of compounds or materials with many distinguishable sites. A polycrystalline sample, e.g., which contains two sites with combined hyperfine interactions will produce 66 major frequencies ($1/2 \rightarrow 3/2$, M1). In such cases, the applicability of SMS depends on ways to impose restrictions on the possible number of frequencies, e.g., by favorable choice of direction of polarization and external fields. Therefore, precise measurements on well-defined systems benefit most from the capabilities of SMS.

The asymptotic behavior of the individual techniques for small effective thickness suggests that SMS is less suited for thin absorbers. However a more careful assessment should consider the measured effect and the available intensity. If statistical errors limit the accuracy, a satisfactory estimate for the quality of the measurement is obtained by taking the product of the square root of the intensity and the effect. For a conventional Mössbauer spectrum, the effect is the ratio of depth of the absorption dip and baseline. The situation is quite different for SMS because there is no such baseline and the effect is only limited by detector noise, which adds to the delayed signal. Assuming small effective thicknesses, SMS produces a higher quality if $\eta^2 > (16\sqrt{C})/\lambda/S$, where C is the ratio of relevant spectral flux for radioactive source to synchrotron radiation, S is the ratio of synchrotron radiation flux in the natural linewidth to detector noise, and $\lambda < 1$ accounts for electronic absorption in the sample. With the numbers given in Table 1 and a detector noise of 0.01 Hz, the condition becomes $\eta\sqrt{\lambda} > 0.02$, and therefore determination of hyperfine parameters with SMS can be advantageous even for highly absorbing samples. However, we would like to emphasize that these conclusions were reached by assuming identical data collection times. A calculation of the delayed flux is presented in fig. 2,

[4]It can be argued that nuclear absorption as observed in conventional Mössbauer spectroscopy occurs promptly whereas only the truly coherent process of "nuclear forward scattering" is delayed.

which can be used to estimate counting rates in experiments.

Phonon excitations. – In previous PHOENIX experiments, the absorption of x-rays from the 14.413 keV nuclear resonance of ^{57}Fe and the subsequent de-excitation by emission of K-fluorescence radiation was observed. Nuclear resonances that are low in energy usually have a very narrow energy width, 4.66 neV for ^{57}Fe. Considering inelastic scattering, one may benefit from such a well-defined energy reference in the lattice. This allows tuning the energy of the incident x-rays with respect to this resonance and not with respect to the energy of the scattered particle, which then would have to be determined. Furthermore, the de-excitation of the nucleus by emission of a conversion electron followed by fluorescence radiation takes place on a time scale of the lifetime of the nuclear resonance, 141 ns for ^{57}Fe. If the nucleus is excited by pulsed synchrotron radiation, the discrimination of nuclear resonant absorption from the electronic contribution is very efficiently done by counting only delayed fluorescence photons. Tuning the energy of the incident synchrotron radiation with respect to the nuclear resonance while monitoring the total yield of the delayed fluorescence photons provides a superposition of all possible phonon excitations.

It was pointed out by Lipkin [29] that certain sum rules would apply to PHOENIX spectra. If $S(E)$ is the inelastic response, the first moment $\int E\,S(E)\,dE$ gives the recoil energy of the free nucleus. This relation was successfully applied to normalize the measured data [22], which then provides $1 - F$. The second moment is proportional to the average kinetic energy of the nucleus and therefore provides an absolute value for the second-order Doppler shift. However the PHOENIX method is based on an incoherent absorption process, and we will always obtain average values. Fingerprinting methods benefit most if the individual compounds are characterized first and results then enter the evaluation of the Mössbauer measurement. In the case of materials with distinguishable sites, additional tools like Mössbauer spectroscopy, x-ray diffraction, and EXAFS have to be employed for an exhaustive characterization. Fig. 3 shows the Lamb-Mössbauer factor and the second-order Doppler shift versus temperature for polycrystalline hematite.

One quite unique application of the PHOENIX method is the study of vibrational dynamics in thin films. In recent experiments at the Advanced Photon Source, ^{57}Fe-rich layers with thicknesses down to 1 nm were investigated. These studies indicate that atomic selectivity in combination with an excellent signal-to-noise ratio will support measurements on ^{57}Fe-tracer layers or measurements with diluted systems containing resonant nuclei. Although ^{57}Fe remains the "preferred choice," other isotopes with low-energy nuclear transitions. listed in Table 2, are feasible for PHOENIX experiments.

Instrumentation. – Applications of nuclear resonant scattering with synchrotron radiation, like SMS and PHOENIX, require instruments that are not common to conventional Mössbauer spectroscopy. Detectors and optical elements constitute the two two major groups of instruments, and they play different roles for SMS and PHOENIX. A typical experimental setup is given in fig. 4. In SMS, the detector, including the timing electronics, is of paramount importance because the precise shape of the time spectrum has to be obtained. The optical elements are merely reducing the photon flux of the powerful

"white", i.e., untreated, synchrotron radiation while keeping the spectral flux at the energy of the nuclear resonance as high as possible. In the case of PHOENIX experiments, the optical elements take over the central role because their energy resolution, tunability, and stability directly affect the quality of the data. The detector collects the delayed events integrated over time, which somewhat relaxes the requirements.

Traditionally x-ray and γ-ray detectors with good time resolution consisted of a combination of a scintillator, which converts the radiation to visible light, and a photomultiplier, which converts the visible light to an electrical current. This design was very elegantly modified by Metge et al. [30] to accommodate the particular needs of nuclear resonant scattering experiments. However, the potential of more intense synchrotron radiation sources was clearly limited by such detector systems, and avalanche photodiodes have mostly supplanted the traditional scintillator-photomultiplier combination for nuclear resonant scattering. Avalanche photodiodes were originally designed for detection of very low light levels, but Kishimoto [7] discovered their value for the time-resolved detection of x-rays. At present, avalanche photodiodes are commonly used for SMS as well as PHOENIX because they combine very good time resolution ($\approx$1 ns), excellent dynamic range ($> 10^9$), and very low noise ($\approx$0.01 Hz). The devices are manufactured with areas up to 200 mm^2 and thus permit one to cover relatively large solid angles. The counting rates should not exceed typically 10^8 Hz to prevent impairment followed by destruction.

Monochromators with high energy resolution are the most valued optical components for both methods. The monochromatization of the "white" synchrotron radiation is usually accomplished in two steps. each by using Bragg or Laue reflections in perfect single crystals made of silicon or diamond. The first monochromator is optimized to handle most of the power in the beam providing an energy resolution of typically 10^{-4}. The second monochromator provides excellent energy resolution, typically 10^{-6} to 10^{-7}. The overall efficiency of the monochromator combination is of the order of 10 % depending on the particular design. Monochromators at the Advanced Photon Source achieved 0.7 meV energy bandwidth at 14.413 keV corresponding to an energy resolution of $5 \cdot 10^{-8}$ [31]. In this bandwidth, a photon flux of $3 \cdot 10^8$ Hz was obtained.

In addition, the development of optical elements filtering one linear polarization to 5 parts in 10^7 by Toellner et al. [32] permits investigation of polarization-dependent SMS. With a set of two "crossed" filters, effects like Faraday rotation are directly observable. The instrument also removes very efficiently nonresonant scattering contributions. Other elements that have not yet been introduced to SMS but may well lead to interesting applications are phase-plates. which convert linear polarization to circular polarization, and focusing optics. Toroidal mirrors can focus the beam to about 0.1×0.3 mm^2 with little reduction in photon flux. A focal spot size of about 10×10 μm^2 is obtainable, however a reduction in flux by a factor 100 has to be accepted. All these devices require the excellent collimation of the synchrotron radiation.

Outlook. – In the last decade, we observed the development of nuclear resonant scattering with synchrotron radiation from observation of the phenomenon to everyday application. What started on a shoestring budget at a bending magnet beamline at HASYLAB, Ger-

many, now counts on continuous support of the largest synchrotron radiation facilities. The ESRF (France), APS (USA), and SPring-8 (Japan) entertain beamlines dedicated to development and application of nuclear resonant scattering techniques. The integrated development of synchrotron radiation optics, detectors, and methods, as well as intense synchrotron radiation sources, provided the push to make nuclear resonant scattering attractive for many scientists. Our present paper illustrated these points. Among the many evolutionary projections that can realistically be made, we would like to suggest the following topics. The relevance of SMS may be extended by introducing polarization filtering and by the use of circularly polarized radiation. An improvement of the energy resolution would directly affect PHOENIX measurements and alleviate detector problems for SMS. Efficient focusing would permit the investigation of very small amounts of material. The study of the coherent inelastic contributions to nuclear resonant scattering may result in development of momentum-resolved PHOENIX. In summary, it appears very likely that continuing development of instruments as well as methods will further the potential of applications of nuclear resonant scattering with synchrotron radiation.

The present work was supported by the U.S. Department of Energy BES-Materials Science under Contract No. W-31-109-ENG-38.

References

[1] E. Gerdau and U. van Bürck, in: Resonant Anomalous X-Ray Scattering : Theory and Applications, eds. G. Materlik, C.J. Sparks, and K. Fischer, (Elsevier, Amsterdam, 1994) and references therein

[2] G.V. Smirnov, Hyp.Int. **97-98**, 551 (1996)

[3] E. Gerdau, R. Rüffer, H. Winkler, W. Tolksdorf, C.P. Klages, and J.P. Hannon, Phys.Rev.Lett. **54**, 835 (1985)

[4] S.L. Ruby, J. de Phys. **35**, C6-209 (1974)

[5] R. Rüffer and A.I. Chumakov, Hyp.Int. **97-98**, 589 (1996)

[6] E.E. Alp, T.M. Mooney, T. Toellner, and W. Sturhahn, Hyp.Int. **90**, 323 (1994)

[7] S. Kishimoto, Rev.Sci.Instr. **63**, 824 (1992)

[8] A.Q.R. Baron and S. Ruby, Nucl.Instr.Meth. A **343**, 517 (1994)

[9] T.S. Toellner, W. Sturhahn, E.E. Alp, P.A. Montano, and M. Ramanathan, Nucl.Instr.Meth. A **350**, 595 (1994)

[10] G. Faigel, D.P. Siddons, J.B. Hastings, P.E. Haustein, J.R. Grover, J.R. Remeika, and A.S. Cooper, Phys.Rev.Lett. **58**, 2699 (1987)

[11] T.M. Mooney, T.S. Toellner, W. Sturhahn, E.E. Alp, and S.D. Shastri, Nucl.Instr.Meth. A **347**, 348 (1994)

[12] A.I. Chumakov, J. Metge, A.Q.R. Baron, H. Grünsteudel, H.F. Grünsteudel, R. Rüffer, and T. Ishikawa, Nucl.Instr.Meth. A **383**, 642 (1996)

[13] T.S. Toellner, M.Y. Hu, W. Sturhahn, K. Quast, and E.E. Alp, Appl.Phys.Lett. , accepted for publication

[14] W. Sturhahn and E. Gerdau, Phys.Rev. B **49**, 9285 (1994)

[15] J.P. Hannon and G.T. Trammell, Phys.Rev. **169**, 315 (1968), Phys.Rev. **186**, 306 (1969)

[16] U. van Bürck, R.L. Mössbauer, E. Gerdau, W. Sturhahn, H.D. Rüter, R. Rüffer, A.I. Chumakov, M.V. Zelepukhin, and G.V. Smirnov, Europhys.Lett. **13**, 371 (1990)

[17] J.B. Hastings, D.P. Siddons, U. van Bürck, R. Hollatz, and U. Bergmann, Phys.Rev.Lett. **66**, 770 (1991)

[18] E.E. Alp, W. Sturhahn, and T.S. Toellner, Nucl.Instr.Meth. B **97**, 526 (1995)

[19] W.M. Visscher, Annals of Physics **9**, 194 (1960)

[20] K.S. Singwi and A. Sjölander, Phys.Rev. **120**, 1093 (1960)

[21] M. Seto, Y. Yoda, S. Kikuta, X.W. Zhang, and M. Ando, Phys.Rev.Lett. **74**, 3828 (1995)

[22] W. Sturhahn, T.S. Toellner, E.E. Alp, X.W. Zhang, M. Ando, Y. Yoda, S. Kikuta, M. Seto, C.W. Kimball, and B. Dabrowski, Phys.Rev.Lett. **74**, 3832 (1995)

[23] A.I. Chumakov, R. Rüffer, H. Grünsteudel, H.F. Grünsteudel, G. Grübel, J. Metge, and H.A. Goodwin, Europhys.Lett. **30**, 427 (1995)

[24] A.I. Chumakov, R. Rüffer, A.Q.R. Baron, H. Grünsteudel, and H.F. Grünsteudel, Phys.Rev. B Rap.Comm. **54**, R9596 (1996)

[25] W. Sturhahn, T.S. Toellner, K.W. Quast, R. Röhlsberger, and E.E. Alp, Rev.Sc.Instr. **67**(9), CD-ROM (1996)

[26] B. Fultz, C.C. Ahn, E.E. Alp, W. Sturhahn, and T.S. Toellner, Phys.Rev.Lett. **79**, 937 (1997)

[27] M. Blume and O.C. Kistner, Phys.Rev. **171**, 417 (1968)

[28] S. Margulies and J.R. Ehrmann, Nucl.Instr. **12**, 131 (1961)

[29] H.J. Lipkin, Phys.Rev. B **52**, 10073 (1995)

[30] J. Metge, R. Rüffer, and E. Gerdau, Nucl.Instr.Meth. A **292**, 187 (1990)

[31] T.S. Toellner, Argonne National Laboratory, unpublished (1997)

[32] T.S. Toellner, E.E.Alp, W.Sturhahn, X.Zhang, M.Ando, Y.Yoda, and S.Kikuta, Appl.Phys.Lett. **67**, 1993 (1995)

property	synchrotron radiation	^{57}Co – source
relevant spectral flux (ph/s/eV)	$2.5{\cdot}10^{12}$	$2.5{\cdot}10^{9}$
brightness (ph/s/eV/sr)	$8.3{\cdot}10^{21}$	$2.5{\cdot}10^{13}$
brilliance (ph/s/eV/sr/mm^2)	$4.0{\cdot}10^{21}$	$2.2{\cdot}10^{7}$
typical beamsize (mm^2)	$1{\times}1$	$10{\times}10$
energy resolution (eV)	variable	$4.7{\cdot}10^{-9}$
energy range (eV)	$7.0{\cdot}10^{-7}$	$\approx 1{\cdot}10^{-4}$
polarization	100 % linear	unpolarized

Table 1: Comparison between a modern synchrotron radiation source and a commercially available ^{57}Co source with 10 mCi activity.

isotope	resonance energy (keV)	half lifetime (ns)	relative strength
^{169}Tm	8.410	4.0	0.38
^{83}Kr	9.4	147	0.2
^{57}Fe	14.4136	97.8	1
^{151}Eu	21.53	9.7	0.63
^{119}Sn	23.87	17.8	6.7
^{161}Dy	25.66	28.1	1.2

Table 2: Isotopes with low energy resonances that are feasible for PHOENIX experiments. The last column gives the relative intensity for the particular isotope compared to ^{57}Fe. It was estimated by $\frac{\sigma\Gamma}{\eta}/(\frac{\sigma\Gamma}{\eta})_{Fe}$, where σ is the nuclear resonant cross section, Γ is the width of the excited nuclear state, and η is the photoelectric cross section.

Figure 1: Reciprocal properties of radioactive sources (top) and synchrotron radiation (bottom) lead to reciprocal experimental techniques. The center panels illustrate the source characteristics averaged over a time period needed for data collection.

Figure 2: Delayed flux versus effective thickness. Eq. 6 was integrated over time starting at 30 % of the half lifetime to account for detector dead time. An incident spectral flux of 10^4 ph/s per natural linewidth was assumed. Mass absorption is not included. The calculation was performed using the CONUSS software.

Figure 3: Lamb–Mössbauer factor (circles) and second–order Doppler shift (triangles) of polycrystalline hematite versus temperature. The values were derived from PHOENIX data taken at the Advanced Photon Source.

Figure 4: Typical experimental setup for SMS (top) and PHOENIX (bottom.) The essential components, detector and optical elements, are discussed in the text.

fig. 1, Sternhalm et al.

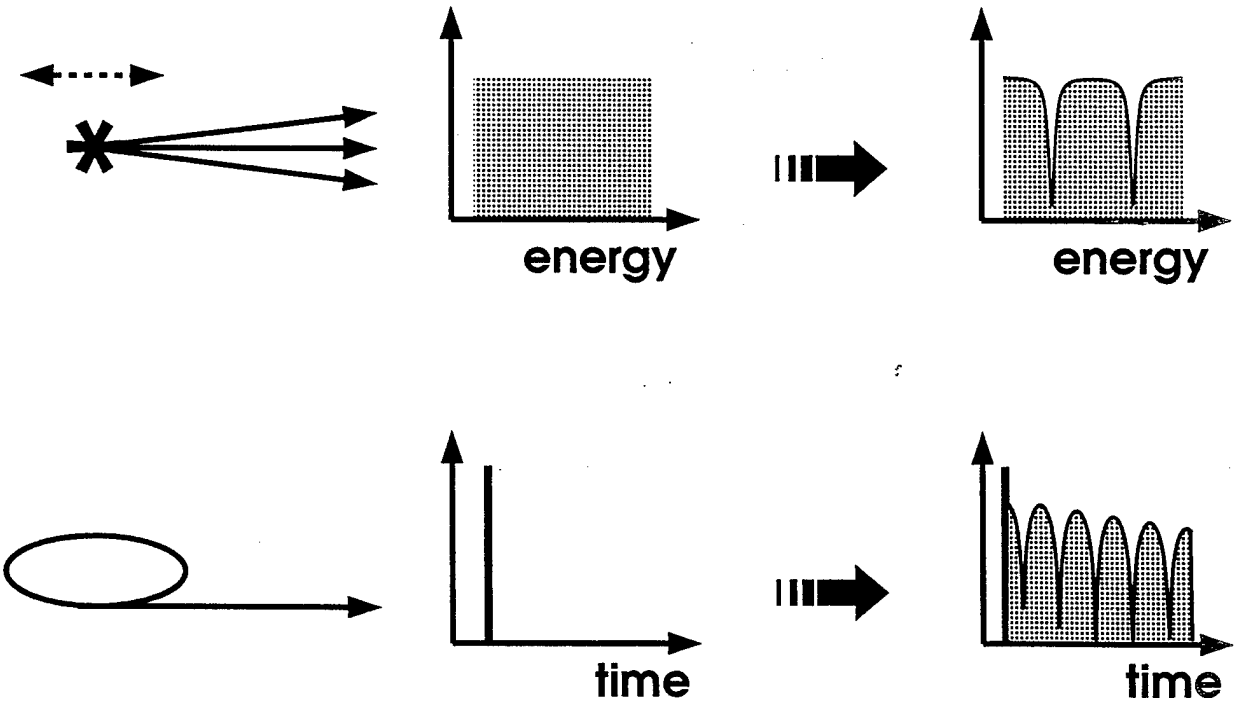

fig. 2, Stenholm et al.

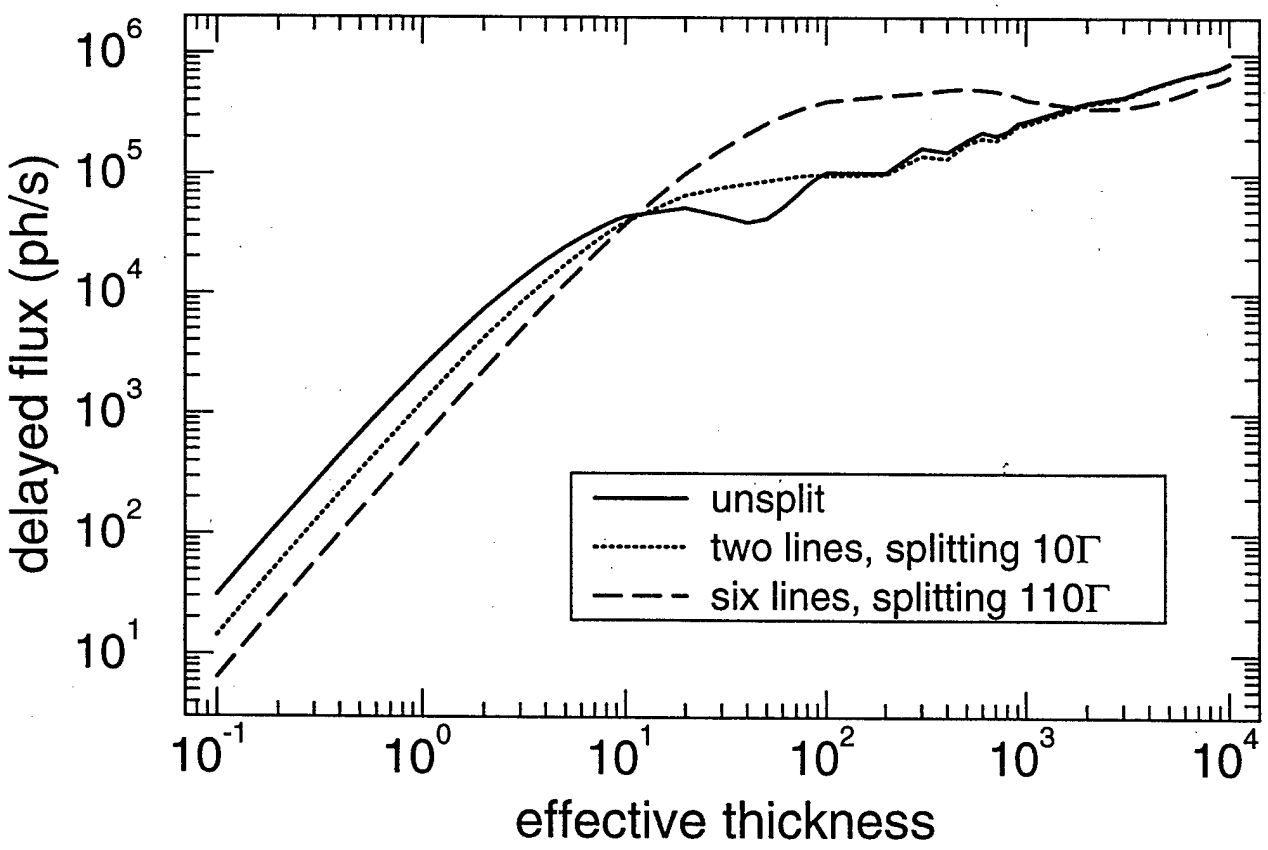

fig. 3, Sturlalun et al.

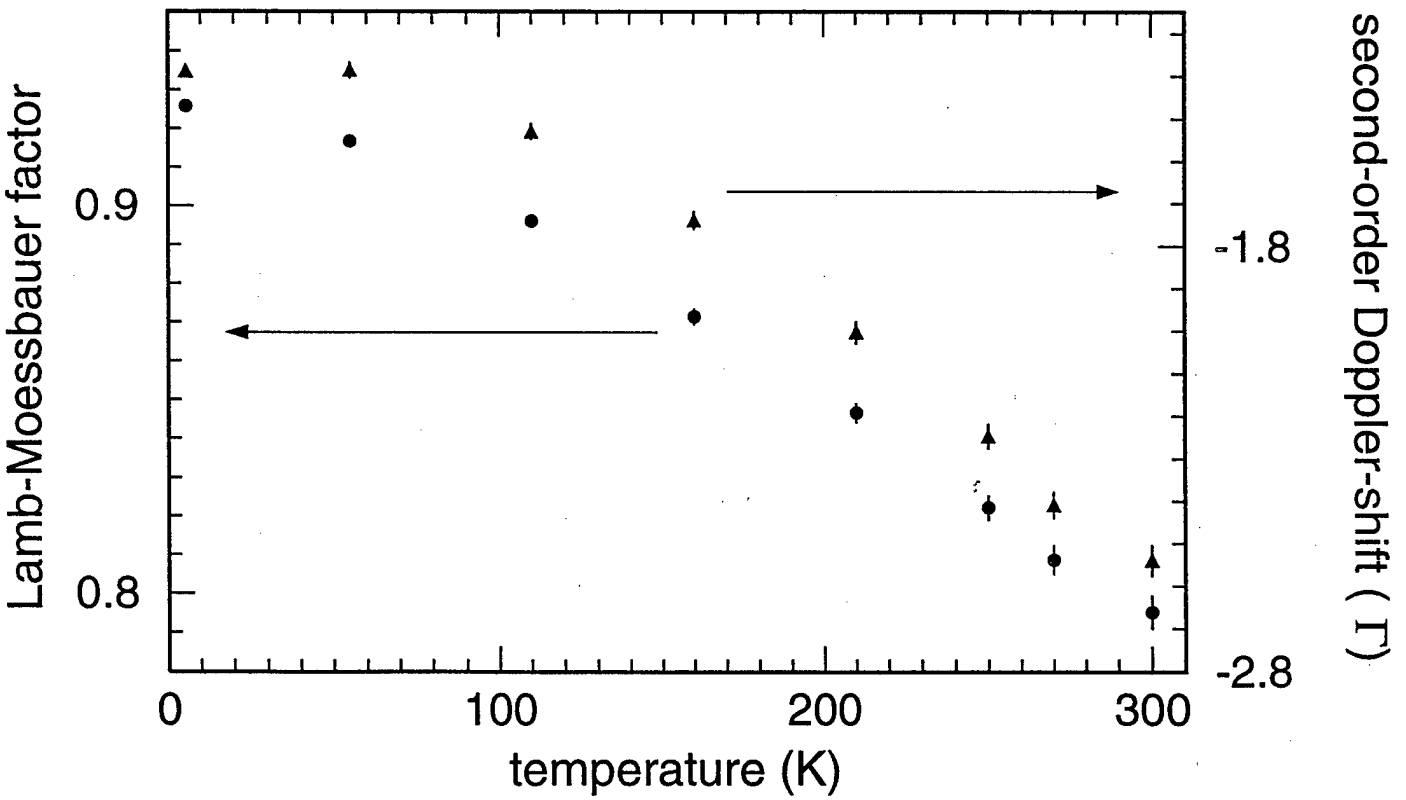

fig. 4, Skurlatov et al.

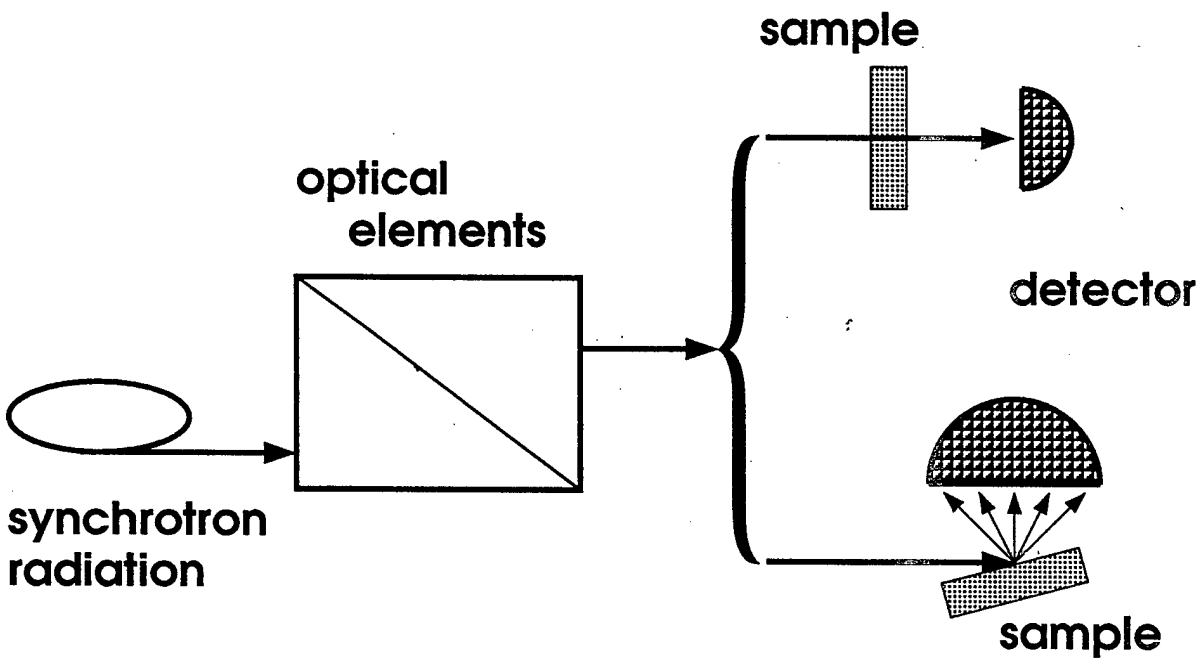

Report Number (14) ANL/XFD/CP--94419
CONF-970916--

Publ. Date (11) 199708
Sponsor Code (18) DOE/ER, XF
JC Category (19) UC-404, DOE/ER

DOE